

Decreased Src Tyrosine Kinase Activity Inhibits Malignant Human Ovarian Cancer Tumor Growth in a Nude Mouse Model¹

Jon R. Wiener,² Kayo Nakano,
Russell P. Kruzelock,³ Corazon D. Bucana,
Robert C. Bast, Jr., and Gary E. Gallick

Departments of Molecular Oncology [J. R. W., R. P. K.], Cancer Biology [K. N., C. D. B., G. E. G.], and Clinical Investigation [R. C. B.], University of Texas, M. D. Anderson Cancer Center, Houston, Texas 77030

ABSTRACT

The Src protein tyrosine kinase is overexpressed and activated in a number of human cancers, including some human ovarian cancers. To determine whether Src activity plays a role in ovarian tumor growth, stable derivatives of the SKOv-3 human ovarian cancer cell line that exhibited reduced Src tyrosine kinase activity were generated by transfection with an antisense *c-src* construct. Comparison of these cell lines with parental SKOv-3 cells and stable sense *c-src* vector-transfected control lines revealed no phenotypic alterations in anchorage-dependent proliferation, adherence, density saturation, or wound migration. However, reduction in Src activity was associated with altered cellular morphology, dramatically reduced anchorage-independent growth, and, when assessed for tumor development in a xenograft nude mouse model, diminished tumor growth. Furthermore, reduction of Src activity in the antisense *c-src* cell lines was associated with reduced vascular endothelial growth factor mRNA expression *in vitro*, and tumors derived from these cell lines displayed a phenotype indicative of abortive microvessel vascularization. These results strongly suggest that Src is involved in critical oncogenic pathways that modulate tumor growth from this ovarian cell line. Furthermore, this evidence suggests that as in other tumor systems, Src activity is required for vascular endothelial growth factor induction and angiogenic development.

INTRODUCTION

Aberrant signal transduction, particularly inappropriate signaling mediated by unregulated tyrosine phosphorylation, is

commonly observed in human tumors. For example, in a significant fraction of human ovarian cancers, the inappropriate expression of the epidermal growth factor receptor PTK⁴ HER-2/*neu* receptor PTK and the macrophage colony-stimulating factor receptor (c-fms) PTK forms the basis for their use as prognostic indicators (reviewed in Ref. 1). Alterations in cellular tyrosine phosphorylation-mediated signaling, resulting in unbalanced total protein phosphotyrosine content, may occur via the overexpression or up-regulation of nonreceptor PTKs as well. The role of nonreceptor PTKs in the development of ovarian tumors remains largely unknown.

The M_r 60,000 pp60^{c-src} nonreceptor PTK (Src) is the prototype member of the Src family of PTKs, all of which are M_r 56,000–62,000 phosphoproteins with intrinsic PTK activity. All nine members of the Src PTK family discovered to date, namely Src, Yes, Fyn, Fgr, Blk, Lck, Lyn, Hck, and Yrk, participate in cell signaling, although the expression and activity of all but Src, Yes, and Fyn are limited primarily to cells of hematopoietic lineage (2). Src is normally involved in cellular functions as diverse as the response to mitogen stimulation, cell cycle control, and cell-cell communication (3). One major function of the Src PTK family is to associate with receptor and nonreceptor PTKs, resulting in the stimulation of tyrosine kinase activity and increased phosphorylation of downstream substrates involved in signaling pathways (4). Indeed, Src activity is required for mitogenesis initiated by the epidermal growth factor receptor and platelet-derived growth factor, two receptor PTKs linked to oncogenic transformation in human tissues (5).

The pp60^{c-src} PTK is expressed in normal ovarian epithelium at relatively low levels. However, we have recently reported that both the expression of the Src protein and intrinsic Src tyrosine kinase activity are significantly increased in human ovarian tumors as well as in cultured human malignant ovarian cancer cell lines.⁵ These results suggest that aberrant Src protein expression and/or kinase activity may also be involved in ovarian tumor development, maintenance, or metastasis. Increased Src protein level and kinase activity are known to be significant contributing factors to early tumor growth in human colon adenocarcinoma (6, 7) and are up-regulated in breast (8, 9) and pancreatic (10) tumors as well. Thus it was of interest to determine whether the up-regulation of Src played a primary role in regulating human ovarian growth, or whether it was an epiphenomenon associated with more fundamental genetic changes that drive the transition to a malignant phenotype. To

Received 2/11/99; revised 5/12/99; accepted 5/17/99.

The costs of publication of this article were defrayed in part by the payment of page charges. This article must therefore be hereby marked *advertisement* in accordance with 18 U.S.C. Section 1734 solely to indicate this fact.

¹ Supported by NIH-National Cancer Institute Grants CA65527 and CA63617 (to G. E. G.), and CA39930 (to R. C. B.).

² To whom requests for reprints should be addressed, at Department of Molecular Oncology, Box 317, University of Texas, M. D. Anderson Cancer Center, 1515 Holcombe Boulevard, Houston, TX 77030. Phone: (713) 792-3790; Fax: (713) 794-1807.

³ Present address: Department of Molecular and Human Genetics, Baylor College of Medicine, 1 Baylor Plaza, Houston, TX 77030.

⁴ The abbreviations used are: PTK, protein tyrosine kinase; VPF, vascular permeability factor; VEGF, vascular endothelial growth factor; FBS, fetal bovine serum; ICKA, immune complex kinase assay; mAb, monoclonal antibody; PECAM, platelet endothelial cell adhesion molecule; TCM, tissue culture medium.

⁵ J. R. Wiener, T. C. Windham, V. C. Estrella, P. Thall, L.-W. Ang, R. C. Bast, Jr., G. B. Mills, and G. E. Gallick. Activated Src protein tyrosine kinase is overexpressed in late stage human ovarian cancer: relationship with Her-2/*neu* expression, manuscript in preparation.

determine the potential role of Src in ovarian cancer tumor growth, we reduced Src expression and activity in the SKOV-3 human ovarian cancer cell line via antisense technology, using an antisense expression vector construct characterized previously (11). This cell line has been well characterized with regard to its use as a model of late-stage human cancer (12, 13) and is representative of ovarian cancer cells that overexpress the HER-2/*neu* PTK (13). In this study, we report that antisense-mediated reduction of Src PTK activity in SKOV-3 malignant human ovarian cancer cells resulted in significantly decreased tumor growth in nude mice, without affecting cellular proliferation. Reduced xenograft tumor growth was accompanied by decreased vascularization of tumor tissues via abortive vessel development. In combination with results that demonstrate that reduction of Src activity resulted in a marked reduction in the expression of VEGF/VPF mRNA levels, our data suggest that Src activity modulates ovarian tumor growth in part by regulating an oncogenic mechanism exclusive of angiogenesis and in part by modulating angiogenic development.

MATERIALS AND METHODS

Reagents. The liposomal transfection reagent LipofectAMINE was obtained from Life Technologies, Inc. (Gaithersburg, MD) and used as directed by the manufacturer. The *c-src* antisense and sense eukaryotic expression vectors used to generate SKOV-3 stable transfectants have been described previously (11). mAb clone 327, which recognizes amino acids 90–120 of Src, was obtained from Oncogene Research Products (Cambridge, MA). mAb clone 1B7 to Yes was obtained from Wako, Inc. (Richmond, VA). The 204-bp cDNA probe for VEGF was obtained as a gift from Dr. Lee Ellis (M. D. Anderson Cancer Center, Houston, TX). [γ - 32 P]ATP (3000 Ci/mmol), [α - 32 P]dCTP (3000 Ci/mmol), and the RediPrime random prime DNA labeling system were obtained from Amersham (Chicago, IL). Rat antimouse CD31 antibody (clone MEC 13.3) against PECAM was obtained from PharMingen (San Diego, CA).

Cell Culture and Transfection. The SKOV-3 human ovarian cancer cell line was obtained from the American Type Culture Collection (Manassas, VA) and maintained in TCM comprised of McCoy5A medium containing 10% heat-inactivated FBS (Sigma, St. Louis, MO), 2 mM L-glutamine (Life Technologies, Inc.), and 20 μ g/ml gentamicin (Life Technologies, Inc.).

Preliminary experiments to determine whether Src expression and activity could be reduced using antisense *c-src* oligonucleotides clearly demonstrated the efficacy of this methodology (data not shown). However, for long-term biological studies, the generation of stable antisense transfectants was deemed to be the most suitable method for specifically reducing Src function. Thus, oligonucleotide linkers encoding either the sense or antisense 40-mer of the *c-src* mRNA sequence enclosing the ATG start codon were cloned into the pcDNA1 vector (11) and used to generate G418/neomycin-resistant SKOV-3 monoclonal lines. For transfection, SKOV-3 parental cells were plated in 100-mm dishes at a density of 1.8×10^4 cells/cm² and, after attachment for 24 h, transfected with 6 μ g of plasmid DNA and 80 μ g of LipofectAMINE, as described by the manufacturer. G418-resistant colonies were selected in 400 μ g/ml G418 (Life Technologies, Inc.), isolated, expanded, and assessed for Src protein expression and intrinsic kinase activity as described below.

Immunoblotting. Immunoblot analysis of prepared cell lysates was performed exactly as described previously (11),

using 250 μ g of total cell protein/lane). Membranes were probed with anti-Src (mAb 327) antibody or anti-Yes (mAb 1B7) and then incubated with horseradish peroxidase-conjugated rabbit antimouse IgG secondary antibodies. Specific binding of the antibody was determined using the enhanced chemiluminescence detection system (Amersham).

ICKA. Monolayer cells in the logarithmic phase of growth were rinsed twice with ice-cold PBS before detergent lysis in modified radioimmunoprecipitation assay buffer containing 20 mM phosphate (pH 7.4), 1% Triton X-100, 150 mM NaCl, 5 mM EDTA, 50 mM NaF, protease inhibitors, and 2 mM sodium orthovanadate. Lysates prepared from solid tumors were homogenized in modified radioimmunoprecipitation assay buffer using a Polytron tissue disrupter (Brinkmann, Inc., Westbury, NY). Clarified lysates (250 μ g of total protein) were reacted with 4 μ g of either mAb 327 for Src immunoprecipitation or mAb 1B7 for Yes immunoprecipitation, and the immune complexes were used in ICKAs as described previously (14). Labeled proteins were separated by electrophoresis on 10% SDS-polyacrylamide gels and detected by autoradiography.

Anchorage-dependent Proliferation Assays. Determination of cell doubling time was performed by plating 6×10^5 cells/60-mm dish in TCM and counting the representative dishes at days 0, 3, and 5. Each time point/cell line was performed in triplicate. Doubling time was calculated using the formula $D_t = (0.69)(t)/\ln M_f - \ln M_i$, where t is time in hours between plating and counting, M_f is the cell number at time t , and M_i is the cell number at time 0. Anchorage-dependent cell proliferation was assessed using the fluorescent CyQuant GR method exactly as described by the manufacturer (Molecular Probes, Junction City, OR). In brief, 5×10^3 cells were plated/well in 96-well tissue culture plates (Nunc, Napierville, IL; eight wells/condition/cell line) and incubated in medium containing the appropriate concentrations of FBS for 24, 48, and 72 h. Quantitation of cell proliferation was performed by measuring fluorescence emission at 520 nm after excitation at 480 nm using a Beckman fluorescent ELISA reader (Beckman, Los Angeles, CA).

Adherence Assay. To measure adherence to the extracellular matrix, collagen IV (Sigma) was plated as described by the manufacturer in 24-well plates (Nunc) and allowed to attach for 1 h at 22°C. The wells were then washed extensively, blocked with 0.2% FBS, and UV sterilized for 10 min. Attachment was initiated by adding 2.5×10^5 cells in 0.5 ml/well and allowed to continue for 3 h at 37°C before staining with PhastGel Blue (Pharmacia, Piscataway, NJ). Quantitative differences in attachment were estimated by visual examination. To measure adherence to plastic surfaces, 2.5×10^4 cells in 0.2 ml of TCM containing either 10% or 0.2% FBS were added per well of 96-well plates (Nunc; four wells/condition/cell line) and allowed to attach for 3 h at 37°C. The medium was then discarded, the wells were washed gently with PBS, and attachment was assessed using CyQuant GR as described by the manufacturer.

Migration Wound Assay. Assessment of wound migration was performed as described previously (15). Briefly, 4×10^5 cells were plated per 35-mm dish (Nunc) and grown to >80% confluence. Wounding of the monolayer was performed by scraping with a sterile tissue scraper, followed by incubation in TCM containing either 10 or 0.5% FBS. After an additional 48 h of incubation, the monolayers were stained with PhastGel Blue and examined visually.

Saturation Density Assay. Determination of cell number at saturation density was performed by plating 2×10^4 cells

in 200 μ l of TCM per well of a 96-well tissue culture plate (Nunc). Cells were allowed to grow to complete confluence and then incubated for an additional 24 h before staining with PhastGel Blue. After extensive washing with PBS, cell density was determined by measuring the proportional stain intensity using absorbance at 490 nm. The mean density for each cell line test group was determined from eight well replicates.

Anchorage-independent Growth Assay. Anchorage-independent (soft agar) cell growth was assessed by planting 2.5×10^4 cells/35-mm tissue culture dish with 2-mm grids (Nunc) in TCM as described previously (16). Each experimental condition was performed in triplicate. Cells were incubated at 37°C in a humidified atmosphere containing 5% CO₂ for 14 days. Colonies that contained ≥ 30 cells were scored.

Xenograft Tumor Growth Assay in Nude Mice. The tumorigenic capability of the antisense and sense *c-src* transfectants was assessed in *nu/nu* mice as described previously (11), with some modification. Briefly, cells were grown to 80% confluence in TCM, harvested by trypsinization, washed twice in HBSS (Life Technologies, Inc.), and resuspended to a final concentration of 2×10^7 cells/ml in sterile PBS containing 33% (v/v) Matrigel (Becton Dickinson). Cell suspensions (0.15 ml) were injected s.c. into the left flank of 6-week-old female *nu/nu* mice. Five mice were inoculated per test group. Tumor volume (in mm³) was calculated using the formula for the volume of a prolate ellipsoid, $(w^2/2)l$, in which *w* and *l* are the width and length of the tumor in millimeters, respectively. Tumors were harvested from exsanguinated mice after 40 days of growth and snap-frozen in OCT compound before CD31/PECAM immunohistochemical staining (see below).

Northern Analysis. Northern analysis for the quantitation of VEGF-specific mRNA was performed as described previously (17). Briefly, the total RNA isolated was electrophoresed (15 μ g/lane) through 1% agarose gels containing 0.22 M formaldehyde. Membranes were probed with radiolabeled VEGF probe in 50% formamide, 5 \times Denhardt's solution, 0.5% SDS, 50 mM Hepes (pH 7.0), 4.8 \times SSC, and 100 μ g/ml salmon sperm single-strand DNA (Sigma) at 42°C for 18 h. Blots were washed in 1 \times SSC containing 0.5% SDS at 22°C and 0.1 \times SSC containing 0.1% SDS at 50°C before autoradiography at -80°C for 3 days with one screen.

Immunohistochemistry. Tumor microvasculature was evaluated immunohistochemically using tumor tissue thin sections harvested from nude mouse xenografts (see above). Tissue sections were fixed sequentially in acetone, acetone/chloroform, and acetone; rinsed in PBS; and endogenous peroxidase-blocked by treating the sections with 3% H₂O₂ in methanol. The sections were then incubated for 20 min at 22°C with a nonspecific protein blocking solution consisting of PBS containing 1% normal goat serum and 1% horse serum. The sections were then incubated with 1:100 primary rat antimouse CD31 antibody at 4°C for 18 h, washed in PBS, and incubated with secondary mAb (peroxidase-labeled mouse antirat antibody; 1:200 dilution; Boehringer Mannheim, Indianapolis, IN) for 1 h at 22°C. After washing, the sections were incubated with stable diaminobenzidine (Research Genetics, Huntsville, AL) for 20 min to develop the peroxidase signal and counterstained with Mayer's hematoxylin (Sigma). Sections were washed and mounted with Universal Mount (Research Genetics) and dried on a hot plate at 60°C before examination.

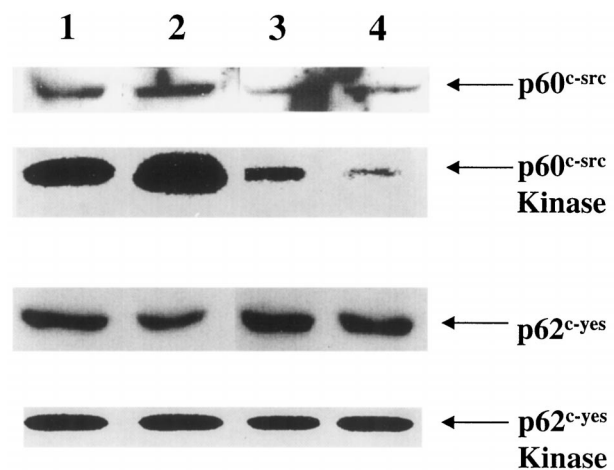


Fig. 1 Western immunoblot analysis and ICKA characterization of *c-src* antisense clones. Immunoblot and immune complex kinase analyses were performed as described in "Materials and Methods." Lane 1, parental SKOV-3 human ovarian cancer cell line; Lane 2, sense *c-src* clone S20; Lane 3, antisense *c-src* clone 2AS4; Lane 4, antisense *c-src* clone AS16.

RESULTS

Phenotypic Characterization of SKOV-3 Transfectants with Reduced Src Activity. Assessment of >50 expanded independent clones by immunoblot assay and ICKA yielded a number of antisense clones that possessed reduced Src tyrosine kinase expression and activity. In particular, the AS16 and 2AS4 antisense clones consistently displayed reduced Src expression or activity (Fig. 1) and were chosen for subsequent study.

The Yes PTK is a member of the Src PTK family that is highly homologous to Src, and it is also expressed at low levels in normal ovarian epithelium relative to the observed overexpression in ovarian cancer cells.⁵ Assessment of the AS16 and 2AS4 monoclonal clones by ICKA for Yes tyrosine kinase activity demonstrated no change in Yes protein expression or intrinsic kinase activity when compared to the parental cell line (Fig. 1) and verified the specificity of the antisense method.

To further characterize the phenotype of the sense and antisense transfectants, cell doubling, wound migration, adherence to plastic or collagen IV, and saturation density were measured. Although the antisense Src transfectants did display altered gross cellular morphology (Fig. 2), no significant difference was observed for any of the other phenotypic properties among the parental SKOV-3 cells and the S20, AS16, or 2AS4 cell lines (Fig. 3A; Table 1).

Reduction of Src Activity Abrogates SKOV-3 Anchorage-independent Growth. The SKOV-3 parental ovarian cancer cell line divides under anchorage-independent conditions to form large colonies (>30 cells) that can be observed visually. A comparison of anchorage-independent growth for the Src transfectants revealed ≈ 700 colonies/35-mm dish for the parental SKOV-3 and sense S20 cells, whereas the two antisense cell lines exhibited diminished capability to grow in soft agar (<35 colonies/dish; Fig. 3B). To address the possibility that the observed reduction in anchorage-independent growth was due merely to clonal variation in the parental SKOV-3 cell line, we isolated single-cell clones of the SKOV-3 parental cell line and performed assays for anchorage-dependent growth and anchor-

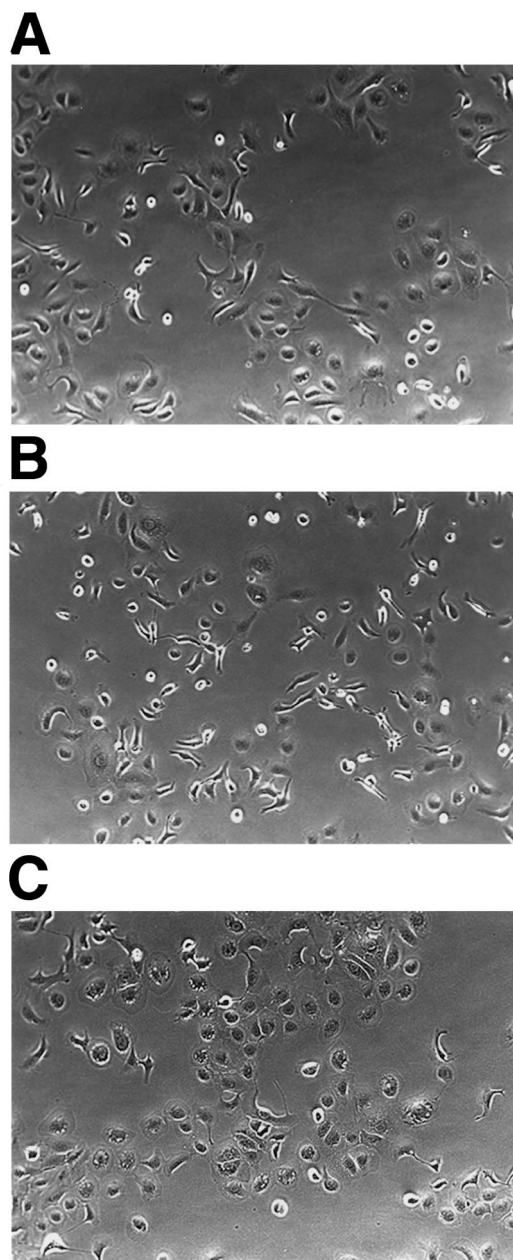


Fig. 2 Gross cellular morphology of *c-src* antisense clone AS16. Photomicroscopy of parental SKOV-3 cells (A), sense *c-src* clone S20 (B), and antisense *c-src* clone AS16 (C). Magnification, $\times 100$.

age-independent growth. Clonal isolates of the parental cell line showed variation in the ability to form colonies in soft agar, ranging between 600 and 1700 colonies/dish; none of the clones displayed the diminished anchorage-independent growth observed in the Src antisense clones (data not shown).

Ovarian Tumor Growth Is Regulated by Src Activity.

To assess directly whether Src activity is involved in *in vivo* tumorigenic growth, the Src transfectants described were used to generate tumors in a nude mouse xenograft model. These stable cell lines were inoculated s.c. into the flanks of 6-week-old

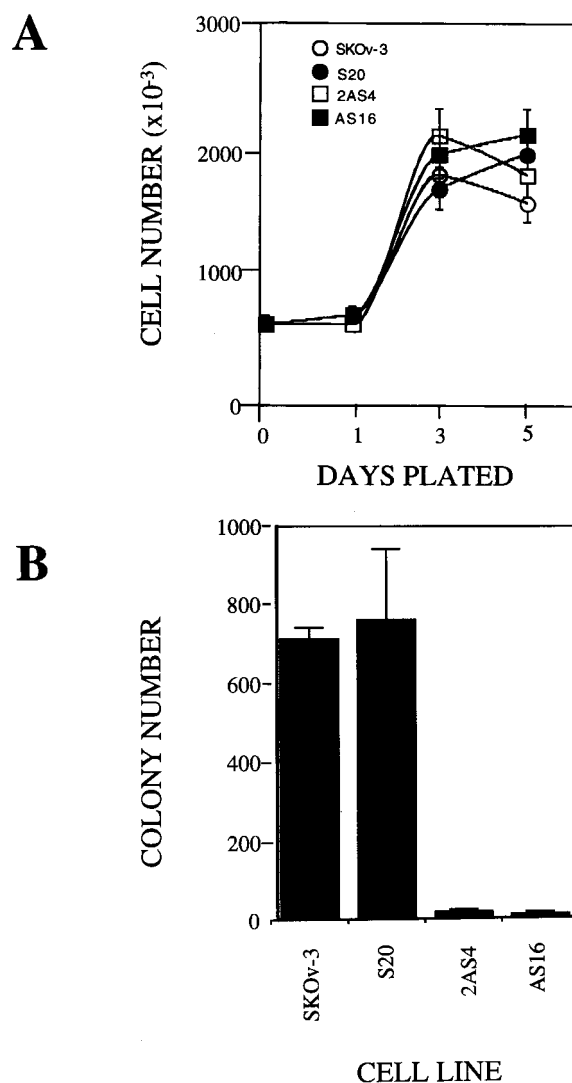


Fig. 3 Analysis of *in vitro* anchorage-dependent and anchorage-independent growth of *c-src* antisense clones. Assays were performed as described in "Materials and Methods." A, anchorage-dependent growth assay; 6×10^5 cells were plated on day 0, and replicate dishes were counted on the days shown. Data from the growth curves were used to calculate doubling times (see Table 1). B, anchorage-independent growth assay; 2.5×10^4 cells were plated, and replicate dishes were examined 14 days after plating for colonies of ≥ 30 cells. *Abscissa*, mean colony number/35-mm dish.

female nude mice, and the tumors were monitored for growth volume as described in "Materials and Methods." Rapid tumor growth was observed for the parental SKOV-3 cells and the sense S20 cells (Fig. 4); by day 32, tumors were large (500–600 mm³) and were beginning to display central necrosis. In contrast, tumors derived from both the 2AS4 and AS16 antisense Src cell lines displayed slower growth kinetics, achieving tumor volumes of only 90–180 mm³ by day 32 (Fig. 4). To assess whether SKOV-3 clonal variation could account for the diminished tumor growth, SKOV-3 clonal isolates of the parental cell line were assessed for tumor growth in the same nude mouse model. All SKOV-3 subclones formed s.c. tumors with a size

Table 1 Phenotypic characterization of SKOv-3 *c-src* transfectants

Cell line	Doubling time (h/days) ^a	Adherence to plastic ^b	Adherence to collagen IV	Saturation density ^c
SKOv-3 (parental cells)	32.2/1.34	45,000 ± 2,600	NOD ^d	0.606 ± 0.074
S20 (sense)	36.4/1.52	36,000 ± 3,500	NOD	0.700 ± 0.061
AS16 (antisense)	34.4/1.43	37,000 ± 1,600	NOD	0.750 ± 0.060
2AS4 (antisense)	26.3/1.10	43,000 ± 2,900	NOD	0.726 ± 0.103

^a Doubling time was calculated using the formula $D_t = (0.69)(t)/\ln M_t - \ln M_i$, where t is time in hours between plating and counting, M_t is the cell number at time t , and M_i is the cell number at time 0.

^b Adherence assays were performed as described in "Materials and Methods." Values shown represent mean fluorescence ± SD, with four replicates/sample. Values shown are in growth medium containing 10% FCS. Similar values were obtained in 0.2% FCS.

^c Saturation density assay was performed as described in "Materials and Methods." Values shown represent mean absorbance ± SD, with eight replicates/sample.

^d NOD, no observable difference between sample groups.

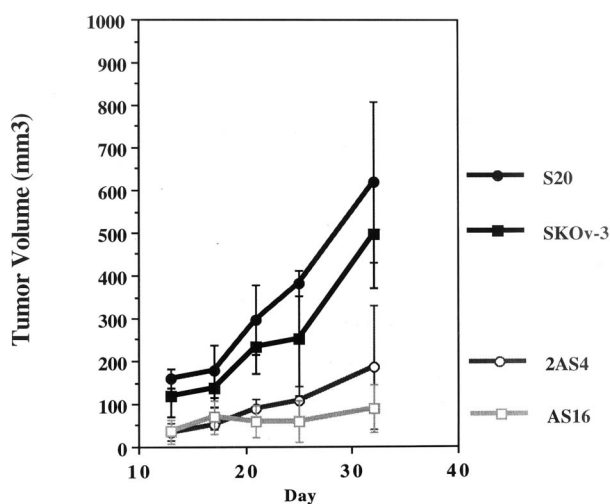


Fig. 4 *In vivo* xenograft tumor growth of *c-src* antisense clones. *In vivo* tumorigenic growth was assessed as described in "Materials and Methods." Replicate groups 6-week-old female nude mice (five mice/group) were inoculated s.c. with 3×10^6 cells in Matrigel in the left rear flank. Tumor growth was monitored by direct measurement, and the volumes (mm^3) were calculated as described in "Materials and Methods."

and growth pattern similar to that of the parental population (data not shown); none displayed the reduced tumor growth observed in the Src antisense clones (data not shown). These data suggest that Src modulates the rate of SKOv-3 ovarian tumor growth *in vivo*.

Analysis of Src kinase activity directly from the mouse tumors verified that the activity was decreased in antisense AS16 and 2AS4 tumors, but not in the parental SKOv-3 or S20 tumor cells. Indeed, the S20 cell line, which generated 17% larger tumors than the SKOv-3 cell line, also displayed a somewhat higher Src activity than the parental cell line (data not shown).

Src Regulates Angiogenic Development in Tumors by Altering VEGF Expression. Src has previously been shown to regulate the expression of the angiogenic factor VEGF/vascular permeability factor in NIH3T3 mouse fibroblasts, 293 kidney cells, and U87 human glioma cells (18) and in colon cancer cells (19, 20). Indeed, Src is required for the hypoxic induction of VEGF (18). In addition, analysis of human ovarian tumors has revealed that high VEGF expression is associated with increased microvessel density and poor overall survival (21, 22). To assess whether a similar mechanism could at least partially explain the reduced ovarian

tumor growth in the antisense *c-src* tumors, we first analyzed VEGF steady-state mRNA expression in the antisense cell lines used for mouse inoculation by Northern blot analysis. Expression of the prominent 3.7-kb VEGF/VPF mRNA was observed to be reduced in the AS16 cell line, as compared to the SKOv-3 parental cell line and the S20 sense control cell line (Fig. 5). These data suggested that Src activity directly regulated VEGF/VPF expression in ovarian cancer cells *in vitro* and suggested further examination of the xenograft tumors for the extent of microvessel development. To this end, the tumors were examined immunohistochemically for CD31/PECAM expression, a marker for endothelial vasculature (20, 23). Visual examination of stained tumor sections from the growing edge revealed that the endothelial vessels in the AS16 tumors displayed diminished branching and decreased vessel thickness (Fig. 6). Numerical counting of endothelial vessels in multiple planes of the tumors revealed that the total number of stained vessels did not differ significantly among the parental, S20, and AS16 tumors (data not shown). These results suggest that reduction of Src expression and activity decreased endothelial vascularization in ovarian tumors, possibly by causing abortive vascular development.

DISCUSSION

Inappropriate activation of the Src PTK has been observed in human carcinomas of colonic (6, 7), breast (8, 9), and pancreatic (10) origin. Indeed, we have recently reported increased Src activity in late-stage human tumors and in a panel of ovarian cancer cell lines.⁵ However, the determination of whether increased Src activity is involved in the regulation of the oncogenic capability of tumor cells must be predicated on a demonstration of diminished tumor growth after the reduction of Src protein kinase activity. In the example presented in this study, we have specifically down-regulated Src kinase activity in the SKOv-3 malignant human ovarian cancer cell line by generating stable transfectants with an antisense *c-src* construct. When compared to the parental cells or to stable sense transfectants, antisense *c-src* transfectants displayed altered morphology, but no significant changes were observed in cellular assays for proliferation, adherence, wound migration, or saturation density. However, the reduction of Src activity in the antisense clones decreased the steady-state expression of VEGF mRNA, dramatically reduced anchorage-independent growth, and sharply curtailed tumor growth in a xenograft mouse model. Finally, reduced tumor growth was coincident with abortive vascular development.

These results strongly suggest that tumor growth in this

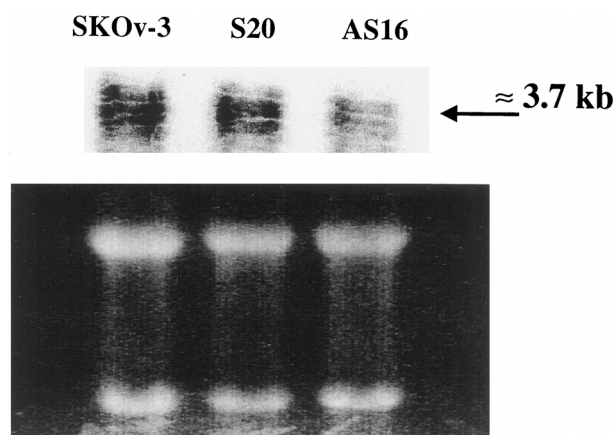


Fig. 5 Northern analysis of steady-state VEGF mRNA expression in *c-src* antisense clone AS16. Analysis of VEGF mRNA expression was performed as described in "Materials and Methods." *Top panel*, autoradiography of membrane probed with ^{32}P -labeled VEGF probe; *bottom panel*, ethidium bromide staining of 1% agarose/formaldehyde gel illustrating equal loading per lane.

model system is at least partially dependent on Src function. Combined with our previous result that Src is overexpressed and activated in human ovarian tumors and cell lines *in vivo*,⁵ our results suggest the possibility that Src has an important, physiologically relevant role in the growth of human ovarian tumors. The mechanism(s) by which Src modulates tumor growth is uncertain at present. Although the reduction in Src did not completely abrogate tumor growth, the dramatic reduction in anchorage-independent growth *in vitro* and the diminished tumor growth *in vivo*, combined with our data showing no observable alteration in anchorage-dependent proliferation *in vitro*, suggest that: (a) Src activity is not essential for normal proliferative functions. This conclusion is in agreement with previous studies using *c-src* knockout mice, in which elimination of functional Src resulted in osteopetrosis but no perinatal lethality, implying that Src is not required for general cell viability due to redundant functional overlap with other Src family PTKs (24); (b) Src activation is vital for the modulation of anchorage-independent growth of human ovarian cancer cells *in vitro*, in agreement with previous studies of colon epithelium (25) or in studies using the activated viral form of Src (26). The dramatic abrogation of anchorage-independent growth in the *in vitro* environment suggests that the activation of Src is essential for oncogenic transformation, although the molecular mechanism(s) that modulates tumor growth and requires Src remains unclear; and (c) Src appears to be involved in the reduced vascularity observed in tumors. The latter phenomenon has been observed in other model tumor systems. Indeed, studies in glioma cells and fibroblasts have revealed that hypoxia induces Tyr⁴¹⁶ phosphorylation and increased Src activity but does not alter Fyn or Yes activity. Furthermore, VEGF induction by hypoxia is significantly impaired by overexpression of dominant-negative *c-src* and in Src⁻ fibroblasts derived from *c-src* knockout mice (18). Whereas these studies remain to be performed in ovarian cancer cells, they strongly suggest that VEGF production, and thus the stimulation of vascular development, is at least partly dependent on Src activation. However, at the present time, we cannot completely eliminate the alternative

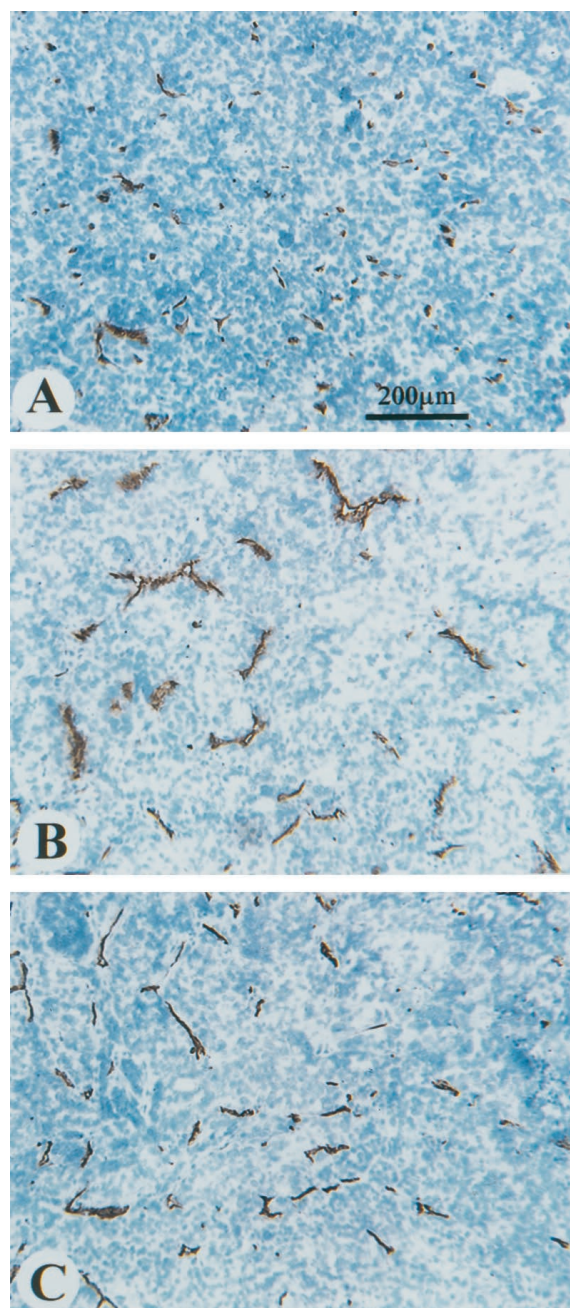


Fig. 6 Immunohistochemical analysis of CD31/PECAM expression in nude mouse tumors from *c-src* antisense clone AS16. Analysis of endothelial vasculature staining in thin sections from mouse tumors was performed as described in "Materials and Methods." Staining was performed on thin sections of tumors derived from *c-src* antisense clone AS16 (A), *c-src* sense clone S20 (B), and parental SKOv-3 ovarian cancer cells (C).

possibility that decreased microvessel development is independent of Src activation.

Increased expression and activation of Src in late-stage ovarian tumors and cell lines suggest that Src activation is a frequent event, albeit following the multiple genetic events that are required for the complex transition from normal ovarian

